

Possible coexistence of rotational and ferroelectric lattice distortions in rhombohedral $\text{PbZr}_x\text{Ti}_{1-x}\text{O}_3$

Marco Fornari

*Center for Computational Materials Science, Naval Research Laboratory, Washington, DC 20375
and Institute for Computational Sciences and Informatics, George Mason University, Fairfax, Virginia 22030*

David J. Singh

Center for Computational Materials Science, Naval Research Laboratory, Washington, DC 20375

(Received 30 June 2000; published 6 February 2001)

The competitions between ferroelectric and rotational instabilities in rhombohedral $\text{PbZr}_x\text{Ti}_{1-x}\text{O}_3$ near $x=0.5$ are investigated using first-principles density-functional supercell calculations. As expected, we find a strong ferroelectric instability. However, we also find a substantial R -point rotational instability, close to but not as deep as the ferroelectric one. This is similar to the situation in pure PbZrO_3 . These two instabilities are both strongly pressure dependent, but in opposite directions so that lattice compression of less than 1% is sufficient to change their ordering. Because of this, and local stress fields due to B -site cation disorder may lead to coexistence of both types of instability are likely present in the alloy near the morphotropic phase boundary.

DOI: 10.1103/PhysRevB.63.092101

PACS number(s): 77.84.Dy

Rhombohedral $\text{PbZr}_x\text{Ti}_{1-x}\text{O}_3$ (PZT) ceramic alloys with compositions near the morphotropic phase boundary (MPB) around $x=0.52$ form the basis of most piezoelectric transducer devices.¹ This is due to a combination of high response, realizable strains in the tenths of % range and favorable weak temperature dependencies.^{2,3} Recently, there has been renewed scientific interest in these materials, driven partly by the discovery of nearly order-of-magnitude higher performance in related relaxor single crystals,^{4,5} and partly by the fundamental understanding of them, being obtained by experimental investigation and first-principles calculations.

The microscopic physics underlying the low-temperature phases of the end points is well known. In PbTiO_3 ferroelectricity is due to condensation of a Γ_{15} unstable phonon where the oxygen octahedra shift against the cations. The ground-state structure has shifts along (001) with a tetragonal lattice strain that stabilizes this direction. A rhombohedral ferroelectric (FE) phase with (111) shifts is not favored and does not occur because of the large electronic hybridization between Pb and O, as may be seen by comparison with BaTiO_3 , which has a rhombohedral FE ground state.⁶⁻⁸

PbZrO_3 has a complex antiferroelectric ground state⁹⁻¹² that may be viewed as arising from the ideal cubic perovskite structure by a combination of strong zone-boundary instabilities.^{13,14} Significantly, the ferrodistorptive Γ_{15} mode that gives the FE ground state of PbTiO_3 is also found strongly unstable in density-functional (DF) studies of cubic perovskite PbZrO_3 even though the ground state is not FE. Also the instabilities of cubic perovskite PbZrO_3 are much stronger than for PbTiO_3 , with energies of 0.20–0.25 eV per formula unit.^{12,15} The actual structure arises from a delicate balance between modes characterized as octahedral rotations, octahedral distortions, and off centering. With the addition of small amounts of Ti, the PZT phase diagram shows a transition to FE behavior, in other words freezing in of the Γ_{15} instability. However, the actual situation is no doubt more complex than this. First of all, in the Zr rich part of the phase

diagram, there is a low-temperature rhombohedral phase in addition to the high-temperature phase characterized by the pure Γ_{15} displacement. This low-temperature phase is associated with a coexistence of the frozen in Γ_{15} FE instability with rotations of the oxygen octahedra.^{2,16,17} Second, local probes indicate a complex local structure that differs substantially from the average diffraction structure in Zr rich PZT and also in the related Pb based relaxor single crystals.^{5,18-20}

Complete phonon dispersions of cubic perovskite PbTiO_3 and PbZrO_3 determined by DF calculations were reported by Ghosez *et al.*²¹ Both materials show both FE (Γ_{15}) and rotational (R_{25} type) instabilities, though in the titanate the rotational (R_{25}) instability is weak and occurs only in small regions of the zone around the R and M points. As mentioned, the R_{25} unstable mode consists of rotation of the oxygen octahedra around the transition metal. The rapid upward dispersion away from R and M is notable; it reflects the rigidity of the octahedra. In cubic perovskite structure PbZrO_3 the R_{25} mode is more unstable and disperses upwards from R weakly, implying more deformable octahedra, a point that was associated with pressure dependencies.²² It should, however, be noted that in materials like PbZrO_3 where the ideal structure is highly unstable, the size of the various instabilities is not simply related to the magnitudes of the corresponding imaginary phonon frequencies in the cubic structure. For example, the phonon frequencies indicate that the R and M point instabilities associated with octahedral rotation in PbZrO_3 are much more unstable than the FE Γ_{15} mode,^{14,21} but, energetically, the FE mode is more unstable.^{12,15}

Here, we use a simple ordered supercell with composition $x=0.5$ to investigate the relative strengths of the FE and rotational instabilities in this region. We find that the FE instability is stronger, as expected, but only marginally so, and that the balance between these may be easily switched by modest strains at the sub 1% level. Noting the difference in ionic radii of Ti and Zr (and the cell volumes of PbZrO_3 and PbTiO_3) and that there is no evidence for cation ordering

TABLE I. Calculated supercell vibrational frequencies (cm^{-1}) of phonons compatible with rhombohedral symmetry.

a_L (a_0)							
7.555	125i	16i	158	326	357	538	838
7.631	122i	33i	150	334	341	500	805
7.708	143i	64i	137	317	324	465	764

in PZT near the MPB,²³ one may conclude, first of all, that these two types of instability may coexist in alloys near the MPB and, second, that it may be helpful to build rotational degrees of freedom into effective Hamiltonians.

We focus on the rhombohedral side of the MPB neglecting the rhombohedral strain that is known to be very small in contrast to the tetragonal phase.²⁴ The supercell used to model the alloy is a ten atom fcc cell with alternating Ti and Zr layers along the $[111]$ direction. This is the same as one of the cells used by Sági-Szabó *et al.*⁸ to investigate piezoelectricity on the tetragonal side of the MPB and Ramer *et al.* to investigate microscopic stress fields.^{25,26} The present DF calculations were done within the Hedin-Lundqvist local-density approximation (LDA) using the general potential linearized augmented plane-wave method²⁷ with local orbital extensions to relax linearization errors and treat semicore states.²⁸ The Brillouin-zone samplings were done using $4 \times 4 \times 4$ special \mathbf{k} -point meshes (note this is for the doubled perovskite cell). Well converged basis sets of over 1650 functions were used with sphere radii of 2.0, 1.83, 2.25, and $1.47 a_0$ for Zr, Ti, Pb, and O, respectively. Forces were calculated by the method of Yu *et al.*²⁹

Calculations were done for three lattice parameters in 1% increments, i.e., 7.555, 7.631, and $7.708 a_0$. While the ideal low-temperature cubic perovskite structure cannot be accessed experimentally, Jaffe *et al.*³⁰ report an effective (by cell volume in the tetragonal phase) value of $7.73 a_0$ at room temperature, while Noheda *et al.*³¹ obtain $7.69 a_0$ for both the tetragonal (slightly above room temperature) and monoclinic (20 K) phases at a slightly more Zr rich composition, $x=0.52$. Within the LDA we obtain a slightly smaller effective lattice parameter for the supercell: $7.55 a_0$, with cubic symmetry (but including the O breathing), and $7.59 a_0$ with a full relaxation into the ferroelectric structure. Such 1–2% smaller lattice parameters relative to experiment are typical of LDA errors in this class of materials.^{12,32} In the ideal cubic structure, the supercell has one internal parameter corresponding to breathing of the octahedron around Ti. At $a = 7.631 a_0$ relaxation of this gives an energy gain of 33 mRy (all energies are for the ten atom cell) with a $0.116 a_0$ reduction of the Ti-O bond lengths—very close to what would be expected ($0.11 a_0$) based on the difference in Ti and Zr ionic radii. This isotropic breathing corresponds to the highest phonon branch as shown in Table I. The frequency of 805 cm^{-1} is higher than that calculated in either pure PbZrO_3 or PbTiO_3 (725 and 612 cm^{-1} , respectively),²¹ as can be expected from bond length considerations (note that the O is between a Zr and Ti yielding a short relaxed Ti-O bond length).

We computed the remaining phonons compatible with a

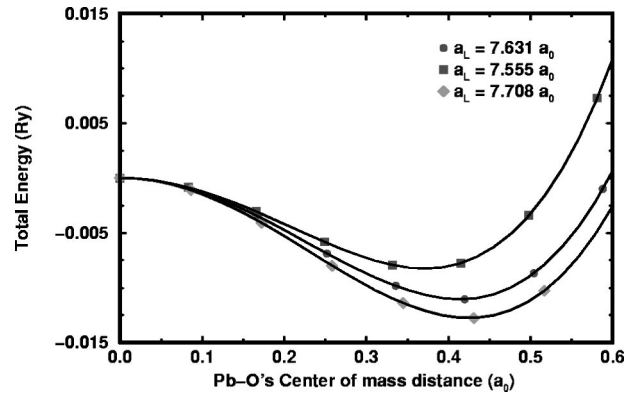


FIG. 1. Relaxation along the FE unstable mode (energies for ten atom supercells) for the reference volume (circles), 1% compression (squares), and 1% expansion (diamonds). The instability decreases under pressure.

rhombohedral symmetry (these are the Γ_{15} and zone folded R_{15} modes of the simple cubic perovskite) from atomic forces for a variety of small distortions about the breather fcc structure. The dynamical matrix was determined by least-squares fit to these, and then diagonalized to obtain the phonon eigenvectors and frequencies (given in Table I) for the three volumes. Additionally, we calculated the energetics of the simple perovskite R_{25} rotational mode (which, however, is not strictly speaking a true pure mode for the fcc supercell). We note that the ferroelectric and rotational modes and the Γ_{15} and folded R_{15} modes belong to different symmetries and therefore do not mix at the harmonic level (e.g., the ferroelectric mode breaks inversion).

The 500-cm^{-1} mode in Table I involves mainly O displacements, like the breathing mode: small octahedra tilting mixed with stretching along $[001]$. The other modes above 300 cm^{-1} involve distortions of the O octahedra, while the lowest stable mode involves mainly transition-metal off centering in the octahedra. In rhombohedral symmetry there is also one marginally unstable and one unstable mode—the R_{15} mode and the FE Γ_{15} instability, respectively. In the ideal perovskite cell and the true disordered alloy, they belong to the same phonon branch and a rough interpolation suggests that the FE instability extends over the entire Brillouin zone as expected by comparison with the full dispersion curve in PbZrO_3 .²¹

Energy minimization along the FE eigenmode at $a = 7.631 a_0$ yields an energy gain of 11 mRy (again per doubled cell). The local minimum compatible with rhombohedral symmetry, however, occurs away from this line and the relaxation provides further energetic gain of 7 mRy. Its coordinates³³ compare well with the displacement pattern obtained by Sági-Szabó *et al.* for the tetragonal FE state (note that at the harmonic level the tetragonal and rhombohedral eigenvectors are the same).⁸ As shown in Fig. 1, the instability is energetically disfavored by compression and favored by expansion. Over the range of 2% in lattice parameter we find a variation of the energy gain along the FE eigenmode of about 5 mRy. Further, the variation in depth of the local minima are larger: 11, 18, and 22 mRy for $a = 7.555 a_0$, $a = 7.631 a_0$, and $a = 7.708 a_0$, respectively.

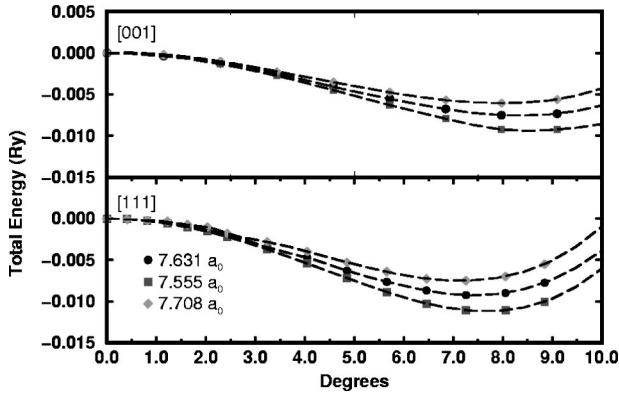


FIG. 2. Variation of the energy (of 10 atom supercells) with ‘rotation’ (a) around [111] and (b) around [001], for the reference lattice parameter (circles), under compression (squares) and under tensile stress (diamonds), as in Fig. 1.

The precise mechanism of the high electromechanical response in PZT and the related relaxor crystals is still not fully established but there are strong indications that polarization rotation from rhombohedral to tetragonal and the strong strain coupling for the tetragonal direction are the main ingredients.^{34–36} Recently, it has been suggested both theoretically³⁶ and experimentally³⁷ that the monoclinic phase found at the MPB (Ref. 31) can bridge the tetragonal and the rhombohedral phase favoring such polarization rotation. Bellaiche *et al.*³⁶ used an effective Hamiltonian approach adapted to the alloy with parameters determined from first-principles calculations. The effective Hamiltonian used allowed strains, alloy disorder, and off-centering displacements to interact, but octahedral rotations were not included. Nonetheless, excellent agreement with experimental data was obtained for the temperature and composition dependence of the piezoelectric and structural properties in PZT, except that the temperature scale had to be uniformly adjusted downwards by approximately one-third.

The microscopic mechanism that makes polarization rotation occur at modest field strengths is still somewhat uncertain though the importance of Pb chemistry has been widely recognized.^{8,12,21,38,39} In particular, it is not fully understood how the instabilities present in PbTiO_3 and PbZrO_3 are modified in the alloy and the extent to which they compete or perhaps coexist in real samples.

Certainly, the simple supercell discussed above is a rather severe approximation to the disordered alloy. Even though Zr and Ti have the same valence, their ionic sizes and electronic properties differ significantly. At the very least, local stresses related to Zr-Ti disorder should be expected in PZT alloys. Zr rich local regions will be under compressive stress so the volume available for the Pb ions is reduced thus lowering the local FE tendency. Ionic considerations, supported by experimental evidence,⁴⁰ predict that octahedral rotations should respond in the opposite way to compression especially if the octahedra are stiff. Consider such rotations around [001] (C_{4h} symmetry) and [111] (C_{3i} symmetry). As mentioned, these are not true modes for the supercell, but they are zone boundary rotational modes that play a key role in at least PbZrO_3 . Both these rotations are unstable (Fig. 2).

At $a = 7.631 a_0$, the energy gain for the [111] rotation is 9 mRy (7 mRy around [001]). It is remarkable that the sizes of the FE and rotational instabilities are so similar for this $x = 0.5$ supercell, considering that they are also quite close, again with the FE instability lower, for PbZrO_3 though with a much higher energy scale. Presumably, they track each other across the rhombohedral side of the phase diagram. This can be qualitatively understood in terms of ionic size effects. Unlike BaTiO_3 or KNbO_3 ,^{41,42} the ferroelectric mode in these Pb based materials is best described as a Pb off-centering with respect to the surrounding O with a smaller transition metal displacement in the same direction. This is clearly seen, e.g., in the Γ_{15} phonon eigenvector. Thus the FE instability is controlled by the volume available to the Pb ion; the rotational mode also involves changes in Pb-O bond length, again controlled by the same distances.

However, a 1% compression (to $a = 7.555 a_0$) increases the rotational instabilities to 11 mRy about [111] and 9 mRy around [001]. Qualitatively, this is related to the stiffness of the O octahedra, especially around Ti; under pressure the octahedra size and geometry can only be retained by rotation, which is made at the expense of the relatively soft Pb-O interaction. This driving force is clearly absent for the FE instability. Experimental evidence of opposite stress dependencies of rotational (R_{25}) and FE (Γ_{15}) instabilities was discussed for PbZrO_3 early on.⁴⁰ Stress-field response calculations²⁵ for $\text{PbZr}_{0.5}\text{Ti}_{0.5}$ supercells suggest that competition between different distortions may be important when uniaxial stress is not parallel to the FE distortion. Considering the different experimental cell volumes of the end points [effective $a(\text{PbZrO}_3) = 7.7883 a_0$ and $a(\text{PbTiO}_3) = 7.5028 a_0$],^{43,44} local stresses sufficient to tip the order of the FE and rotational instabilities seem quite reasonable in the disordered alloy. As noted, the FE instability occurs at the Γ and R points and probably over most or all of the zone. Thus it can occur on a very local scale in real space. The rotational instability is no doubt more localized in reciprocal space, so several octahedra must rotate in concert within a region, but this region may be realizable small, as the ZrO_6 octahedra may be soft as in PbZrO_3 providing weak connections in the interlinked network. In this scenario, coexistence of rotational and FE distortions in the alloy is expected. The resulting disorder might increase response away from the MPB, though at the expense of maximum attainable response at the best composition—this would be favorable for obtaining a desirable weak temperature dependence of the response. In any case, it is clear that rotational degrees of freedom are in the low energy space along with the FE mode, and presumably should be considered in the construction of effective Hamiltonians, either via explicit additional coordinates or renormalization of the existing FE and strain related coordinates. This could possibly improve the temperature scale.

We thank R. E. Cohen, L. Bellaiche, T. Egami, and B. Burton for helpful discussions. The code FINDSYM by H. T. Stokes and L. Boyer was used for some symmetry analysis. This work was supported by ONR and the DoD ASC computer center.

- ¹K. Uchino, *Piezoelectric Actuators and Ultrasonic Motors* (Kluwer Academic, Boston, 1996).
- ²B. Jaffe, W. R. J. Cook, and H. Jaffe, *Piezoelectric Ceramics* (Academic Press, New York, 1971).
- ³M. E. Lines and A. M. Glass, *Principles and Applications of Ferroelectrics and Related Materials* (Clarendon, Oxford, 1977).
- ⁴S.-E. Park and T. R. ShROUT, J. Appl. Phys. **82**, 1804 (1997).
- ⁵T. Egami, W. Dmowski, M. Akbas, and P. K. Davies, in *First Principles Calculations for Ferroelectrics*, edited by R. Cohen (AIP, New York, 1998), Vol. 436, p. 1.
- ⁶R. E. Cohen, Nature (London) **358**, 137 (1992).
- ⁷U. V. Waghmare and K. M. Rabe, Phys. Rev. B **55**, 6161 (1997).
- ⁸G. Sághi-Szabó, R. E. Cohen, and H. Krakauer, Phys. Rev. B **59**, 12 771 (1999).
- ⁹H. Fujishita and S. Katano, J. Phys. Soc. Jpn. **66**, 3484 (1997).
- ¹⁰H. Fujishita and S. Katano, Ferroelectrics **217**, 17 (1998).
- ¹¹S. Teslic and T. Egami, Acta Crystallogr., Sect. B: Struct. Sci. **B54**, 750 (1998).
- ¹²D. J. Singh, Phys. Rev. B **52**, 12 559 (1995).
- ¹³H. Fujishita and S. Hoshino, J. Phys. Soc. Jpn. **53**, 226 (1984).
- ¹⁴W. Zhong and D. Vanderbilt, Phys. Rev. Lett. **74**, 2587 (1995).
- ¹⁵D. J. Singh, Ferroelectrics **194**, 299 (1997).
- ¹⁶D. Viehland, J. F. Li, X. H. Dai, and Z. Xu, J. Phys. Chem. Solids **57**, 1545 (1996).
- ¹⁷D. L. Corker, A. M. Glazer, R. W. Whatmore, A. Stallard, and F. Fauth, J. Phys.: Condens. Matter **10**, 6251 (1998).
- ¹⁸W. Dmowski, M. K. Akbas, P. K. Davies, and T. Egami, J. Phys. Chem. Solids **61**, 229 (2000).
- ¹⁹T. Egami, W. Dmowski, M. Akbas, and P. K. Davies, Ferroelectrics **436**, 1 (1998).
- ²⁰S. Teslic, T. Egami, and D. Viehland, J. Phys. Chem. Solids **57**, 1537 (1996).
- ²¹P. Ghosez, E. Cockayne, U. V. Waghmare, and K. M. Rabe, Phys. Rev. B **60**, 836 (1999).
- ²²E. Cockayne and K. M. Rabe, J. Phys. Chem. Solids **61**, 305 (2000).
- ²³C. A. Randall, A. S. Bhalla, T. R. ShROUT, and L. E. Cross, Ferroelectr. Lett. Sect. **11**, 103 (1990).
- ²⁴R. W. Whatmore and A. Glazer, J. Phys. C **12**, 1505 (1979).
- ²⁵N. J. Ramer, E. J. Mele, and A. M. Rappe, Ferroelectrics **296**, 31 (1998).
- ²⁶N. J. Ramer and A. M. Rappe, J. Phys. Chem. Solids **61**, 315 (2000).
- ²⁷D. J. Singh, *Planewaves, Pseudopotentials and the LAPW Method* (Kluwer Academic, Boston, 1994).
- ²⁸D. Singh, Phys. Rev. B **43**, 6388 (1991).
- ²⁹R. Yu, D. J. Singh, and H. Krakauer, Phys. Rev. B **43**, 6411 (1991).
- ³⁰B. Jaffe, R. S. Roth, and S. Marzullo, J. Res. Natl. Bur. Stand. **55**, 239 (1955).
- ³¹B. Noheda, D. E. Cox, G. Shirane, L. E. Cross, and S.-E. Park, Appl. Phys. Lett. **74**, 2059 (1999).
- ³²N. Marzari and D. J. Singh, Phys. Rev. B **62**, 12 724 (2000), and references therein.
- ³³The atomic positions of the atoms in the relaxed FE cell are: (0.0, 0.0, 0.0) and (1.0+ δ_{Pb} , 1.0+ δ_{Pb} , 1.0+ δ_{Pb}) for Pb's (1.5+ δ_{Zr} , 1.5+ δ_{Zr} , 1.5+ δ_{Zr}) for Zr (0.5+ δ_{Ti} , 0.5+ δ_{Ti} , 0.5+ δ_{Ti}) for Ti (0.5+ δ_{O1}^x , 0.5+ δ_{O1}^x , 0.0152+ δ_{O1}^z), (0.5+ δ_{O1}^x , 0.0152+ δ_{O1}^z , 0.5+ δ_{O1}^x) (0.0152+ δ_{O1}^z , 0.5+ δ_{O1}^x , 0.5+ δ_{O1}^x), (0.5+ δ_{O2}^x , 0.5+ δ_{O2}^x , 0.9848+ δ_{O2}^z), (0.5+ δ_{O2}^x , 0.9848+ δ_{O2}^z , 0.5+ δ_{O2}^x), (0.9848+ δ_{O2}^z , 0.5+ δ_{O2}^x , 0.5+ δ_{O2}^x) for the 6 O's. The energy minimum occurs for $\delta_{Pb} = -0.006$, $\delta_{Zr} = 0.032$, $\delta_{Ti} = 0.032$, $\delta_{O1}^x = 0.069$, $\delta_{O1}^z = -0.084$, $\delta_{O2}^x = 0.069$, $\delta_{O2}^z = 0.089$. The coordinates are in terms of the lattice parameter $a_L = 7.631 a_0$.
- ³⁴S. E. Park and T. R. ShROUT, J. Appl. Phys. **82**, 1804 (1997).
- ³⁵H. Fu and R. E. Cohen, Nature (London) **281**, 403 (2000).
- ³⁶L. Bellaiche, A. García, and D. Vanderbilt, Phys. Rev. Lett. **84**, 5427 (2000).
- ³⁷R. Guo, L. E. Cross, S.-E. Park, B. Noheda, D. E. Cox, and G. Shirane, Phys. Rev. Lett. **84**, 5423 (2000).
- ³⁸L. Bellaiche, J. Padilla, and D. Vanderbilt, Phys. Rev. B **59**, 1834 (1999).
- ³⁹B. P. Burton and E. Cockayne, Phys. Rev. B **60**, 12 542 (1999).
- ⁴⁰G. A. Samara, Phys. Rev. B **1**, 3777 (1970).
- ⁴¹R. E. Cohen and H. Krakauer, Phys. Rev. B **42**, 6416 (1990).
- ⁴²D. J. Singh and L. L. Boyer, Ferroelectrics **136**, 95 (1992).
- ⁴³T. Mitsui *et al.*, *Numerical Data and Functional Relationships in Science and Technology* (Springer-Verlag, New York, 1981).
- ⁴⁴E. Sawaguchi, J. Phys. Soc. Jpn. **8**, 615 (1953).